Available online at www.sciencedirect.com
SCIENCE DIRECT®
Catalysis Today 93–95 (2004) 561–566
CATALYSIS TODAY
www.elsevier.com/locate/cattod

Structural transformation of PdPt nanoparticles probed with X-ray absorption near edge structure

Sung June Cho [a,*], Sung Kyu Kang [b]

[a] *National Research Laboratory for Clean Energy Technology, Department of Applied Chemical Engineering and the Research Institute for Catalysis, Chonnam National University, Yong Bong 300, Buk-gu, Gwang-ju 500-757, Republic of Korea*
[b] *Korea Institute of Energy Research, 71-2 Jang-dong, Yusung-gu, Taejon 305-343, Republic of Korea*

Available online 14 July 2004

Abstract

Structural transformation of bimetallic PdPt nanoparticles has been investigated with X-ray absorption near edge structure at high temperatures. PdPt bimetallic nanoparticles have been prepared on a La-doped alumina by a sequential loading of H_2PtCl_6 onto the Pd loaded catalyst. The results of extended X-ray absorption fine structure at Pd K and Pt L_{III} edges showed that Pt was surface-enriched or anchored on the Pd metal core with an increase of the Pt content. The structure of the obtained bimetallic PtPd nanoparticles seemed to be retained upon heating up to 1273 K under ambient condition. The measurement of catalytic activity of these PdPt bimetallic nanoparticles over methane combustion showed that the difference in activity with increasing and decreasing reaction temperatures was disappeared probably due to the synergistic effect of the formation of the PdPt bimetallic nanoparticles.

Keywords: Nanoparticles; Methane; Combustion; Pd catalyst; EXAFS; XANES

1. Introduction

Commercialization of a catalytic combustor using Pd catalyst supported on metal substrate has been underway because of its clean combustion characteristics compared to those of conventional combustion technologies [1]. The Pd catalyst showed the reversible structural transformation from more active PdO to less active Pd or vice versa during high temperature combustion of methane where PdO is known as a major active component [1–3]. Farrauto et al. proposed the structural model of the reversible structural transformation based on the series of the thermo-gravimetric experiment by measuring a weight change of Pd/Al_2O_3 catalyst upon desorption and adsorption of oxygen [4]. During the reversible structural transformation, the Pd catalyst can sinter readily to lose combustion activity. The sintering of the Pd catalyst however can be inhibited employing improved preparation methods; formation of bimetallic nanoparticles and the surface coating with high temperature-resistant metal oxides such as TiO_2 [5] and ZrO_2.

In the previous report [5], we showed the increase of the thermal stability of Pd catalyst with the surface coating of titanium oxide because of the strong metal support interaction between and TiO_2 and Pd nanoparticles [6]. The model for the reversible structural transformation of the Pd catalyst was also suggested based on the result of the data analysis of extended X-ray absorption fine structure and X-ray absorption near edge structure (EXAFS/XANES) as a function of heating temperature. The XANES feature is well known to be sensitive to the oxidation state or electronic structure of X-ray absorbing metal [7]. Thus, a series of the XANES spectra of the Pd catalyst against heating temperatures can show the change of the atomic and electronic structure in the nanoparticles, otherwise it was difficult to obtain.

In this work, we extend our previous work on the reversible structural transformation of the Pd catalyst to the formation of bimetallic nanoparticles with platinum. The model for the reversible structural transformation upon the formation of bimetallic nanoparticle has been suggested with

* Corresponding author. Tel.: +82 62 530 1902; fax: +82 62 530 1909.
E-mail address: sjcho@chonnam.ac.kr (S.J. Cho).

0920-5861/$ – see front matter © 2004 Elsevier B.V. All rights reserved.
doi:10.1016/j.cattod.2004.06.106

respect to the effect on the catalytic performance for methane combustion.

2. Experimental

$Pd(NO_3)_2$ (Engelhard, 19.9% Pd) was impregnated into La-doped Al_2O_3 (2 mol% La–Al_2O_3) supplied from Condea Inc. The surface area of La-doped Al_2O_3 was 90 $m^2\,g^{-1}$. The La-doped Al_2O_3 showed rather high thermal stability for example above 1273 K compared to the pure Al_2O_3. The activation procedure was the calcination in oxygen at 823 K for 6 h followed by the reduction with hydrogen at 823 K for 4 h. The Pd loading of the catalyst was controlled to 2 wt% on dry basis. The obtained Pd catalyst was denoted as Pd/La–Al_2O_3.

The formation of PdPt bimetallic nanoparticles was performed as follows: the Pd catalyst was impregnated with the aqueous solution containing the desired amount of H_2PtCl_6. The platinum complex impregnated Pd catalyst was dried in oven at 373 K for overnight. The obtained sample was reduced at 823 K by flowing hydrogen without the activation in oxygen. The platinum loading was controlled to 0.5, 1.0 and 2.0, respectively. The bimetallic catalyst was also denoted as Pt/Pd/La–Al_2O_3.

X-ray absorption measurement was carried out in ambient air using Beamline 10B and 7C at the Photon Factory in Tsukuba. For high temperature measurements, a specially designed XAFS cell with Kapton window (DuPont, 125 μm) was used. The temperature was raised from room temperature to 1273 K. The EXAFS data was analyzed using XFIT and Feff6 [8]. The details of EXAFS data analysis can be found elsewhere [9].

The catalytic activity over the sample was measured using the microreactor system equipped with gas chromatograph (HP5890, Hewlett Packard). The methane concentration was controlled to 1 vol% in 99% air. The space velocity, GHSV was 30,000 h^{-1}.

3. Results and discussion

Microstructure of bimetallic nanoparticles on various supports has been investigated extensively using various characterization techniques. The previous study on the formation of Pt nanoparticles showed that the microstructure of the bimetallic nanoparticle can be controlled easily with a sequential loading of metal components and proper treatments [10,11]. Ryoo and co-workers showed that 2–4 nm sized Pt nanoparticle can be obtained if the $Pt(NH_3)_4^{2+}$ was loaded secondly on the 1 nm Pt particle and subsequently reduced with hydrogen. While, the 1 nm Pt particle was obtained when the secondly loaded $Pt(NH_3)_4^{2+}$ containing sample was subject to oxidation and subsequent reduction. According to their proposed mechanism, the preloaded Pt nanoparticles can be reduced readily with hydrogen near room

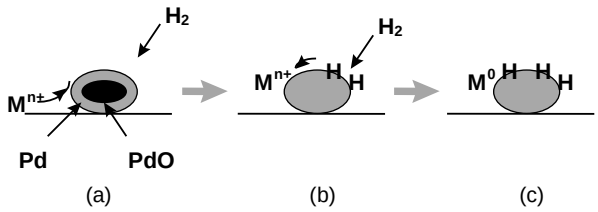

Fig. 1. (a) Initial reduction by hydrogen of the preloaded nanoparticles, (b) the hydrogen adsorption on the nanoparticles and the movement of the secondly loaded metal ions near to the reduced metal nanoparticles and (c) the reduction of the secondly loaded metal ions by the adsorbed hydrogen to form the bimetallic nanoparticles.

temperature. The reduced Pt nanoparticles can adsorb atomic hydrogen which can reduce the secondly loaded metal species readily. Thus, it can be speculated that the secondly loaded metal ions can be reduced near or next to the preloaded metal nanoparticles, resulting in a surface enrichment or a high surface coverage over the preloaded metal nanoparticles. In this manner, many different types of bimetallic nanoparticles can be prepared such as PtAg [12], PtCu [13], PtPd [14], etc.

Combustion activity of methane over Pt is diffusion controlled while not for Pd because of the presence of the reversible structural transformation [1,4]. In order to improve the catalytic performance in methane combustion, the Pd core covered with Pt is preferred due to the difference in the catalytic activity. The reason is that Pd is more thermally stable than Pt. In the present work, the above mentioned mechanism for the formation of bimetallic nanoparticles has been utilized to prepare the microstructure of Pt surface-enriched Pd metal core as illustrated in Fig. 1. The catalytic performance of the PdPt bimetallic nanoparticles prepared on La-doped alumina over methane combustion was compared in Fig. 2 with those of the Pd and Pt catalysts, respectively. The light-off temperature (T_{10}) at which the 10% methane

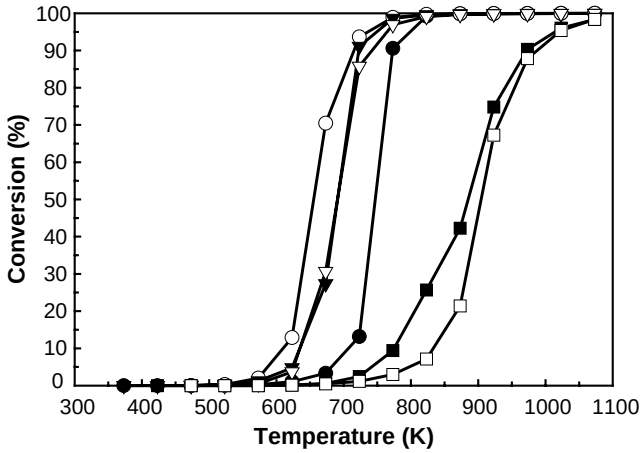

Fig. 2. Catalytic activity of: (circles) 2 wt% Pd/La–Al_2O_3, (rectangles) 2 wt% Pt/La–Al_2O_3, and (triangles) Pt/Pd/La–Al_2O_3 (Pt/Pd = 0.5). The open and closed symbols indicate the increase and the decrease of the reaction temperatures, respectively.

Table 1
Apparent activation energy of the catalysts over methane combustion

Sample	E_a in ramp-up (kJ mol^{-1})	E_a in ramp-down (kJ mol^{-1})
1 wt% Pd/La–Al_2O_3	30.4	44.8
2 wt% Pd/La–Al_2O_3	33.3	49.5
2 wt% Pt/La–Al_2O_3	43.9	43.8
Pt/Pd/La–Al_2O_3 (Pt/Pd = 0.5)[a]	49.9	49.6

The reaction rate was measured under the reactant flow of 1 wt% CH_4 and 99% air with GHSV = 30,000 h^{-1}.

[a] The sample was prepared with the sequential loading method using 2 wt% Pd/La–Al_2O_3 as a parent catalyst.

conversion reached for the Pt catalyst was higher than that of the Pd catalyst by 170 K. Depending on the combustion temperature, the Pd catalyst also showed a large activity difference because of the reversible structural transformation [15]. The temperature for the reversible structural transformation of PdO to Pd can be distributed from 923 to 973 K depending on the supports, the presence of dopant like La^{3+} or metal oxides like NiO, metal particle size, etc. [16,17].

The obtained PdPt bimetallic catalyst showed a unique catalytic performance. There was no catalytic activity difference when the temperature was ramp-up and ramp-down against the reaction temperatures. Such reaction data implied no significant structural change during methane combustion. Table 1 showed the apparent activation energy of methane combustion for the catalysts. The PdPt bimetallic nanoparticles showed the same apparent activation energy as that of the Pd catalyst, 49 kJ mol^{-1}, with increasing and decreasing reaction temperatures. The apparent activation energy for the Pd only catalyst upon the ramp-up of the reaction temperature was 33 kJ mol^{-1}, implying to the presence of highly active PdO state. Thus, the apparent activation energy of methane combustion for the PdPt nanoparticles suggested that the incorporation of Pt into the Pd catalyst change the state of Pd by the formation of bimetallic nanoparticles.

Fig. 3 shows the X-ray absorption near edge structure (XANES) of Pd foil and PdO at the Pd K edge. At the Pd K edge, the absorption transition at 24,348 eV is 1s → 4d dipole forbidden transition according to the selection rule, $\Delta l = 1$ and $\Delta j = 1$, where l and j are the orbital angular momentum and the total angular moment of the local density of states. This transition intensity is suppressed greatly as shown in Fig. 3(a). The absorption cross-section in the K edge region of transition metals is strongly influenced by d–s, p hybridization because the unoccupied bands are d bands. Thus, in system where the d–s, p hybridization is strong, the p-like density of states is strongly enhanced and the absorption can be increased like the second and third absorption peaks in the XANES spectrum of Pd foil. The XANES spectrum of PdO showed the strong absorption at the Pd K edge since the d–p hybridization of Pd^{2+} increased significantly the absorption cross-section, compared with that of Pd foil.

Thus, the XANES spectra for Pd and PdO standard materials thus have characteristic features which are sensitive to the change of physico-chemical environment of the absorbing atom, such as the change of oxidation state, hydrogen chemisorption, the formation of bimetallic particles, etc. In the previous work, the reversible structural transformation of Pd catalyst during the thermal cycling in ambient air was monitored following the XANES feature at the Pd K edge [5].

The significant difference can also be found in the XANES spectra for the PdPt bimetallic nanoparticles as shown in Fig. 3(b). Upon the increase of the Pt content, the near edge

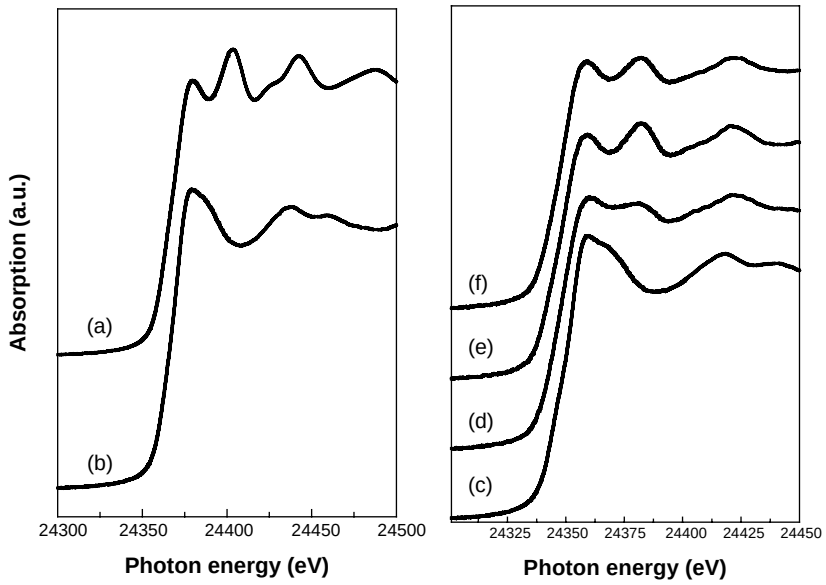

Fig. 3. Near edge spectra of the: (a) Pd foil, (b) PdO, (c) Pt/Pd/La–Al_2O_3 (Pt/Pd = 0.0), (d) Pt/Pd/La–Al_2O_3 (Pt/Pd = 0.5), (e) Pt/Pd/La–Al_2O_3 (Pt/Pd = 1.0) and (f) Pt/Pd/La–Al_2O_3 (Pt/Pd = 2.0) at the Pd K edge. The absorption inflection corresponds to 1s → 4d transition. The second and third peaks correspond to dp and dsp transitions, respectively.

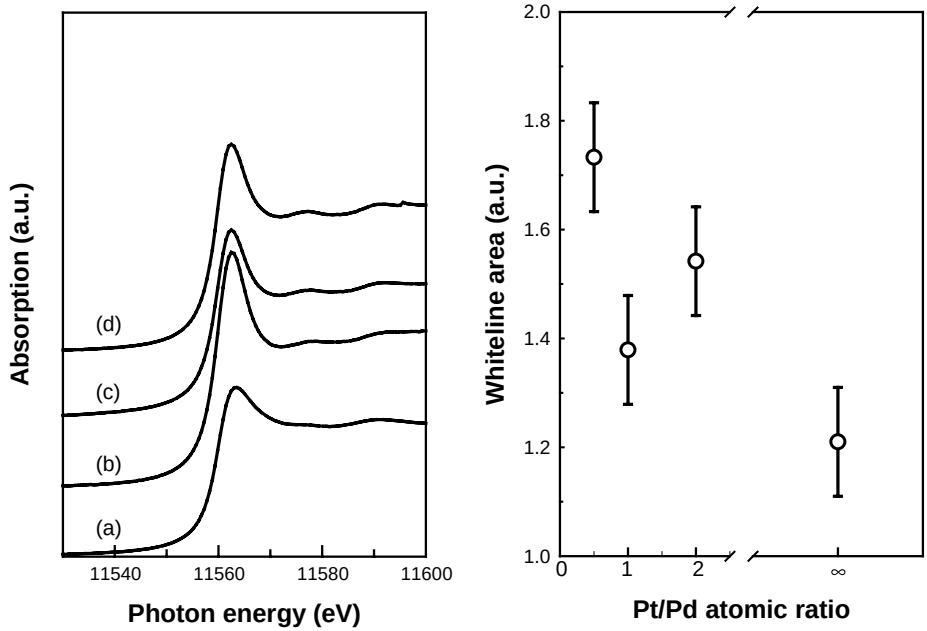

Fig. 4. Left panel: near edge spectra of the: (a) Pt foil, (b) Pt/Pd/La–Al_2O_3 (Pt/Pd = 0.5), (c) Pt/Pd/La–Al_2O_3 (Pt/Pd = 1.0) and (d) Pt/Pd/La–Al_2O_3 (Pt/Pd = 2.0) at the Pt L_{III} edge. Right panel: the Whiteline area plotted as a function of Pt/Pd ratio. The Whiteline area was obtained form the curve fitting with the combination of the Lorentz and arctangent functions.

structure at the Pd K edge changed progressively to resemble to that of Pd foil. At a high loading of Pt, the XANES spectrum was almost the same as that of Pd foil probably due to the surface enrichment of Pt over the Pd metal, thereby inhibiting the interaction between Pd and oxygen.

The Whiteline area in the XANES of the PdPt bimetallic nanoparticles at the Pt L_{III} edge decreased as shown in Fig. 4 with the increase of the Pt content, which implied the decrease of the electron vacancy in d band of the Pt atom. Since both $2p_{3/2} \rightarrow 5d_{3/2}$ and $2p_{3/2} \rightarrow 5d_{5/2}$

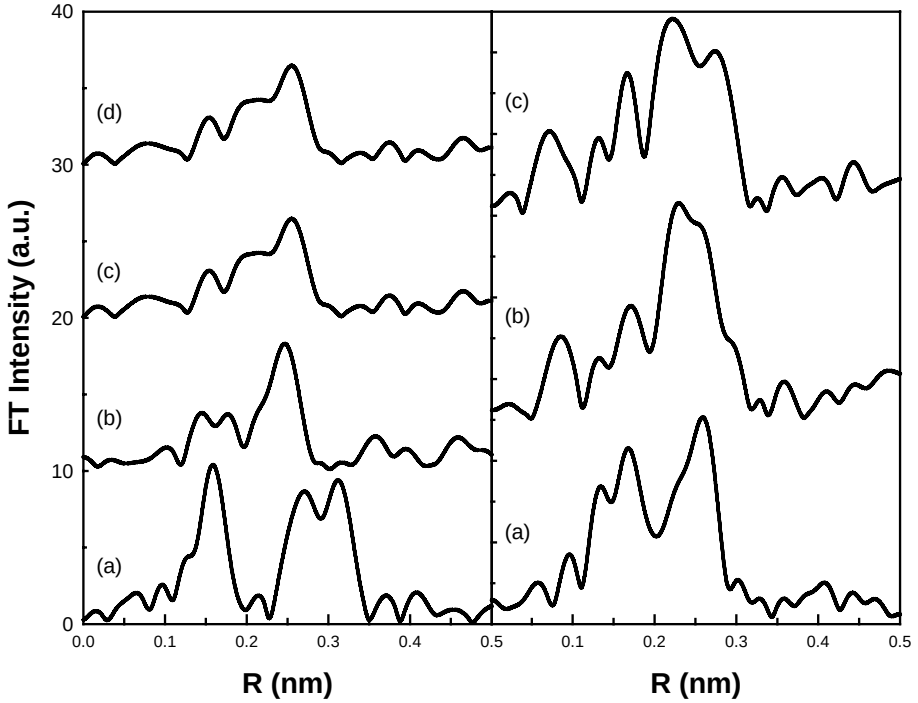

Fig. 5. Left panel: Fourier transforms of the k^3-weighted EXAFS spectra of: (a) Pt/Pd/La–Al_2O_3 (Pt/Pd = 0.0), (b) Pt/Pd/La–Al_2O_3 (Pt/Pd = 0.5), (c) Pt/Pd/La–Al_2O_3 (Pt/Pd = 1.0) and (d) Pt/Pd/La–Al_2O_3 (Pt/Pd = 2.0) at the Pd K edge. Right panel: Fourier transforms of the k^3-weighted EXAFS spectra of: (a) Pt/Pd/La–Al_2O_3 (Pt/Pd = 0.5), (b) Pt/Pd/La–Al_2O_3 (Pt/Pd = 1.0) and (c) Pt/Pd/La–Al_2O_3 (Pt/Pd = 2.0) at the Pt L_{III} edge.

Table 2
Structural parameters obtained from the curve fitting of EXAFS data measured above the Pd K and Pt L_{III} edges, respectively

Sample	Edge	Pair	$N \pm 1$	$R \pm 0.001$ (nm)	$\sigma^2 \pm 10$ (pm^2)[a]
Pd/La–Al_2O_3	Pd K	Pd–O	3.5	0.201	17
		Pd–Pd	4.8	0.305	58
		Pd–Pd	4.2	0.343	42
Pt/Pd/La–Al_2O_3 (Pt/Pd = 0.5)	Pd K	Pd–O	2.0	0.201	54
		Pd–Pd	2.7	0.271	56
		Pd–Pt	4.2	0.267	49
	Pt L_{III}	Pt–O	3.4	0.193	142
		Pt–Pd	4.3	0.258	56
		Pt–Pt	4.7	0.259	49
Pt/Pd/La–Al_2O_3 (Pt/Pd = 1.0)	Pd K	Pd–O	–	–	–
		Pd–Pd	5.2	0.273	57
		Pd–Pt	4.2	0.270	73
	Pt L_{III}	Pt–O	1.3	0.201	82
		Pt–Pd	1.7	0.272	38
		Pt–Pt	3.4	0.271	70
Pt/Pd/La–Al_2O_3 (Pt/Pd = 2.0)	Pd K	Pd–O	–	–	–
		Pd–Pd	2.3	0.273	63
		Pd–Pt	7.4	0.270	96
	Pt L_{III}	Pt–O	1.3	0.199	58
		Pt–Pd	1.2	0.272	35
		Pt–Pt	5.1	0.271	70

[a] The Debye–Waller factor.

electronic transitions are allowed at the Pt L_{III} edge, the hole density in the $5d_{5/2}$ and $5d_{3/2}$ state becomes proportional to the Whiteline area, which is more sensitive to the change of electronic structure than that at Pd K edge. The decrease of the Whiteline area with the increase of Pt content suggested the decrease of the electron vacancy resulting from the formation of the PdPt bimetallic nanoparticles.

The results of the data analysis of the EXAFS spectrum of the PdPt bimetallic nanoparticles are presented in Fig. 5 and Table 2. The model structure of the Pd nanoparticles was proposed to be tetragonal PdO consisted of four oxygen atoms at 0.203 nm, eight palladiums at 0.300 nm and four palladium at 0.340 nm [5]. The reduced Pd particles have a coordination number of Pd–Pd, 8.8 at 0.272 nm, indicating the formation of 1–2 nm Pd particles. At the Pd K edge, the oxygen coordination around the palladium atom decreased substantially with the increase of platinum content up to 1.0. The peak at 0.15 nm (not phase shift-corrected) comes from the Pt contribution because of the non-monotonic behavior of the amplitude function of Pt atom. The same peak at similar position was also observed in the Fourier transform of the EXAFS spectrum above the Pt L_{III} edge.

The fraction of Pd–Pt bimetallic pair was increased progressively to 75% for Pt/Pd/La–Al_2O_3 (Pt/Pd = 2.0) with respect to total coordination number, indicating the Pt enrichment at the Pd surface. The overall coordination number was 9 ± 1 at 0.270 nm, implying the reduced state in 2 nm bimetallic nanoparticles. On the other hand, the oxygen contribution to the EXAFS was detected at the Pt L_{III} edge in the series of the PdPt bimetallic nanoparticles consistent with the structure of the Pd metal core covered with Pt atom. The total metal coordination number obtained from Pt EXAFS data was 6 ± 1 with 0.271 nm, indicating the dispersion of Pt atom on the surface of Pd nanoparticles.

Fig. 6 showed the XANES spectra of the PdPt bimetallic nanoparticles as a function of the heating temperatures at the Pd K and Pt L_{III} edges. At Pd K edge, the XANES features were almost the same as that of Pd metal except the slight change near 873 K. At Pt L_{III} edge, the Whiteline area also increased with the increase of the heating temperature up to 873–973 K and decreased again through heating and cooling to 673 K. The oxygen desorption occurred from the metal nanoparticles near 873–973 K, which were shown in our previous report using TPD-MS measurement of effluent gas [5]. Oxygen desorption in the Pd catalyst was resulted in the formation of the surface attached PdO species. Similarly, oxygen desorption can occur in the PdPt bimetallic nanoparticles so that it seems to cause a slight change of the microstructure of PdPt bimetallic nanoparticles. The result of XANES at the Pd K edge and Pt L_{III} edge, however, showed that the PdPt bimetallic nanoparticles maintain a Pt surface-enriched Pd core structure. Thus, it can be suggested that the reversible structural transformation of Pd can be removed by the formation of PdPt bimetallic nanoparticles without sacrificing the catalytic performance in methane combustion. Further studies on the microstructure of the PdPt bimetallic nanoparticles are in progress using the curve

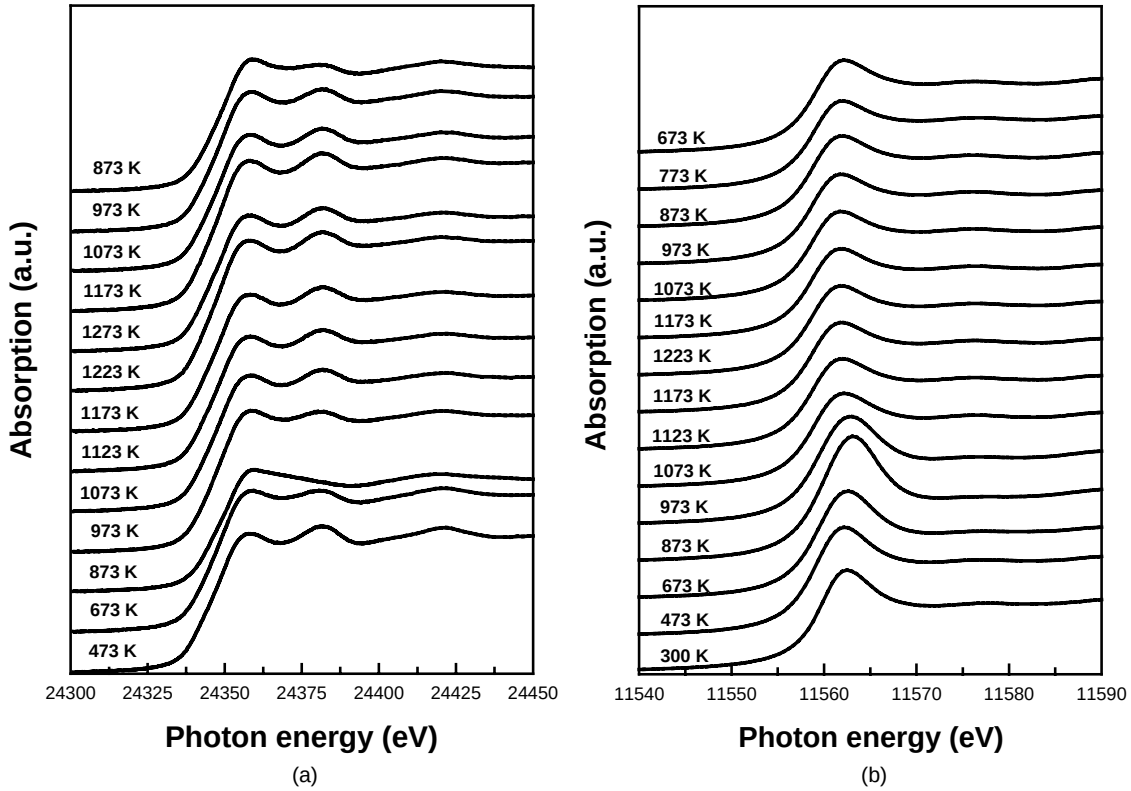

Fig. 6. Near edge spectra of the PtPd bimetallic nanoparticles measured as a function of heating temperatures at: (a) the Pd K edge and (b) the Pt L_{III} edge.

fitting of the EXAFS spectra obtained at the both Pd K and Pt L_{III} edges at high temperatures.

4. Conclusion

The PdPt bimetallic nanoparticles contained its microstructure of the Pd metal core covered with Pt up to 1273 K under ambient condition without the reversible structural transformation. The measurement of catalytic activity of the PdPt bimetallic nanoparticles over methane combustion showed that the structural change of the bimetallic nanoparticles resulted in the removal of hysteric behavior of catalytic activity along heating temperatures. The present work suggested that the XANES has been a very useful technique to measure the change of the oxidation state or microstructure if it is combined with EXAFS and catalysis.

Acknowledgements

This work was supported by the National Research Laboratory Program of the Ministry of Science and Technology, Korea.

References

[1] R.A. Dalla Betta, Catal. Today 26 (1995) 329.
[2] D.L. Trimm, Appl. Catal. 7 (1983) 249.
[3] L. Pfefferle, W.C. Pfefferle, Catal. Rev. Sci. Eng. 29 (1987) 219.
[4] R.J. Farrauto, M.C. Hobson, T. Kennelly, E.M. Waterman, Appl. Catal. 81 (1992) 227.
[5] S.J. Cho, S.K. Kang, J. Phys. Chem. B 104 (2000) 8124.
[6] K. Asakura, J. Inukai, Y. Iwasawa, J. Phys. Chem. 96 (1992) 829.
[7] B. Moraweck, A.J. Renouprez, E.K. Hlil, R. Baudoing-Savois, J. Phys. Chem. 97 (1993) 4288.
[8] (a) J.J. Rehr, R.C. Albers, S.I. Zabinsky, Phys. Rev. Lett. 69 (1992) 3397;
(b) P.J. Ellis, H.C. Freeman, J. Synchrotron Rad. 2 (1995) 190.
[9] D.C. Koningsberger, R. Prins, Principles, Application, Techniques of EXAFS, SEXAFS, and XANES, Wiley, New York, 1988.
[10] R. Ryoo, S.J. Cho, C. Pak, J.Y. Lee, Catal. Lett. 20 (1993) 105.
[11] R. Ryoo, S.J. Cho, C. Pak, J.-G. Kim, S.-K. Ihm, J.Y. Lee, J. Am. Chem. Soc. 114 (1992) 76.
[12] R. Ryoo, C. Pak, S.J. Cho, Jpn. J. Appl. Phys. 32 (Suppl. 2) (1993) 475.
[13] D.H. Ahn, J.S. Lee, M. Nomura, W.M.H. Sachtler, G. Moretti, S.I. Woo, R. Ryoo, J. Catal. 133 (1992) 191.
[14] C. Pak, R. Ryoo, Appl. Mag. Reson. 8 (1995) 475.
[15] A. Ersson, H. Kuar, R. Carroni, T. Griffin, S. Järås, Catal. Today 83 (2003) 265.
[16] H. Widjaja, K. Sekizawa, K. Eguchi, H. Arai, Catal. Today 35 (1997) 197.
[17] K. Eguchi, Catal. Sci. Technol. 12 (1996) 133.